

13-5**3 D Reconstruction of Manufactured Parts using Bi-directional Stereovision-based Contour Matching and Comparison of Real and Synthetic Images**

Aïcha Beya FAR
LSIIT (UMR ULP-CNRS 7005)
Université Louis Pasteur
Bd Sébastien Brant, BP 10413
F-67412 Illkirch-Cedex, France
far@lsiit.u-strasbg.fr

Sophie KOHLER
LSIIT (UMR ULP-CNRS 7005)
Université Louis Pasteur
Bd Sébastien Brant, BP 10413
F-67412 Illkirch-Cedex, France
kohler@lsiit.u-strasbg.fr

Ernest HIRSCH
LSIIT (UMR ULP-CNRS 7005)
Université Louis Pasteur
Bd Sébastien Brant, BP 10413
F-67412 Illkirch-Cedex, France
hirsch@lsiit.u-strasbg.fr

Abstract

Computer vision for industrial applications, such as quality control, inspection, and accurate-measurement tasks leading to quantitative evaluation of machined parts, requires efficient tools for the computation of 3D descriptions of the image contents. Stereovision is one such powerful technique for obtaining 3D information from 2D images. Prerequisite is adequate feature matching. However, most available matching techniques are often not well adapted for images of machined parts. In this paper, thus, an adequate approach for matching features extracted from such images is presented. Rather to rely on single points, it makes use of lines and curvilinear segments as primitives and takes into account the number of points belonging to each edge. Further, the standard epipolar constraint is used twice, from left to right in the stereo image pair and vice-versa, to eliminate false matches. Lastly, a priori knowledge, e.g. the CAD model of the object of interest, is used as a constraint to keep for further processing only contours of the object seen in both images. The approach has been tested on real images and experimental results show that our method produces more accurate contour correspondences and thus better 3D reconstruction.

1 Introduction

For industrial applications of computer vision, such as quality control and accurate measurement tasks leading to quantitative inspection of manufactured parts, it is necessary to develop tools for the accurate computation of 3D descriptions out of the image contents. The latter can then be compared with the CAD model of the object under investigation. Further, the procedures should be fully automated, in order to favor take-up. In this paper, we focus on 3D contour representations. In this case, stereovision is a powerful technique for computing 3D information using 2D image features belonging to the same 3D point in the imaged scene [1], [2], [3]. However, given a point in the first image, finding its correspondent in the other image is a very hard task, still widely discussed in the literature. This problem can be solved by using, as examples, functions similarity measures (e.g., correlation functions) [4] or matching functions based on the constraint implied by the so-called epipolar geometry, with disparity constraints for line matching [5]. In this paper, we suggest an adapted approach for contour matching based on the cross-application of the epipolar

constraint in the stereo pair, and on a comparison between actual and synthetic data in order to select the set of contours to be matched. In section 2, we review the epipolar constraint and then describe in details the different steps of the proposed matching approach. The comparison step between real and reference data is introduced in section 3. Representative experimental results from an actual implementation are parts of both sections 2 and 3. Finally, the contribution is concluded with a short outlook in section 4.

2 Matching Procedure based on a Bi-directional Epipolar Constraint

The geometry of the sensor is composed of two cameras, mounted on an experimental bench (Fig. 1), with distinct viewpoints o_l and o_r . Each one is described by the widely used pinhole model (Fig. 2), associated respectively with the camera matrices, k_l and k_r [2].

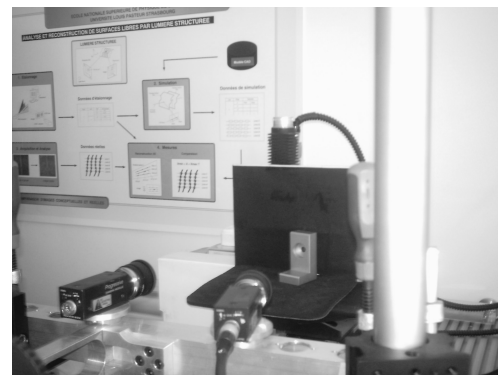


Figure 1. Stereo head.

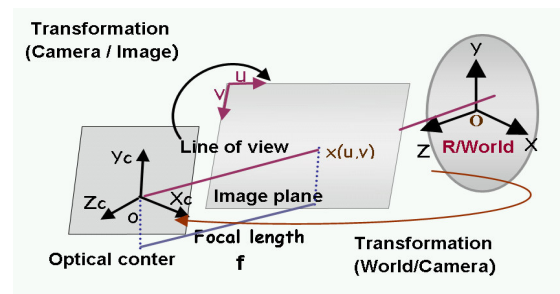


Figure 2. Pinhole camera model.

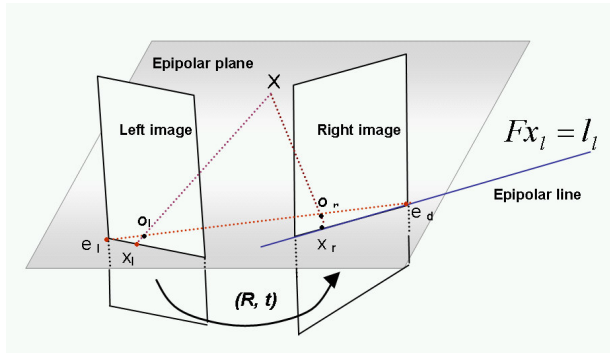


Figure 3. Epipolar geometry.

The 3D point X is imaged as $x_l = k_l \cdot X$ in the left view and $x_r = k_r \cdot X$ in the right one. The epipolar geometry (Fig. 3) describes the intrinsic projective geometry between the two views [6], [7], independently of scene structure, and only depends on the internal parameters of the cameras and their relative positions. The 3×3 fundamental matrix F of rank 2 encapsulates this geometry [1], [6], [7], [8], [15], [16] and is its algebraic representation. Thus, the only available geometric constraint for solving the correspondence problem is this epipolar geometry [1]. Specifically, the correspondent x_l of x_r is constrained to lie on a line, and vice-versa. Thus, for a point in the left image, its correspondent in the right image must lie on this epipolar line. Algebraically, the following equation must be satisfied:

$$x_l \cdot F \cdot x_r = 0 \quad (1)$$

$$\text{With} \quad F = k_l^{-t} \cdot t \cdot R \cdot k_r^{-1} \quad (2)$$

(R, t) is a rigid transformation (rotation and translation), relating the left camera coordinate system to the right one [9]. The equivalent relationship :

$$x_r \cdot F^t \cdot x_l = 0 \quad (3)$$

where F^t is the transpose of F maps points from the right image to the left. In this paper, we use a standard approach known as the “normalized eight point algorithm” [1] to estimate the fundamental matrices.

2.1 Matching procedure

The matching problem is usually solved by using a similarity measure (such as, e.g., a correlation function) between 2 D images. This approach gives rather good results for real world images composed essentially of textured areas. But this technique is often not well adapted for images of machined parts. Our approach for contour matching, based on the epipolar geometry, relies also on computation of similarity criteria. This technique firstly classifies pre-computed lists of contour points as either straight lines or arbitrary shaped contours, using the method described in [10]. This step has two major advantages. Firstly, each image contents is described using much fewer features than available contour points. Secondly, the search for corresponding primitives becomes limited. Accordingly, for each primitive of a given class in the left hand image, we search for a correspondence of the same class in the right hand image.

In our method, we take into account two representations of contours, either as contour points or contour chains, according to [11]. The matching algorithm is presented in detail in the next section for straight lines primitives, the process being the same for the other class of edges.

Given the sets of points $x_{i,l}$ of a contour $C_{i,l}$, $i = \{1, \dots, m\}$, m being the number of primitives in the left image, and $x_{j,r}$ of a contour $C_{j,r}$, $j = \{1, \dots, n\}$, n being the number of primitives in the right image, we seek the correspondences between the two sets of points. Using the fundamental matrix F , the correspondences between the two sets of contour points are determined. But, usually, the epipolar lines lead to several intersections with a given contour. Thus, for all the points $x_{i,l}$ belonging to $C_{i,l}$, we calculate the corresponding epipolar lines and we determine the number of their intersections with all the right primitives. The set of intersections $n_{j,r}$, $j = \{1, \dots, n\}$, provides the initial candidates to be matched with points $x_{i,l}$.

Since these points belong to contour $C_{i,l}$, these are good candidates to be matched with the right contours $C_{j,r}$. A pair of matched contour points thus indicates a possible correspondence between the two contours to which they belong. However, this does not guarantee that no false matches are obtained.

2.2 Elimination of false matches and validation of matches

As a result of the previous stage, a so-called matching matrix is obtained. This matrix summarizes the number of intersections with the right primitives calculated for all the points building the left primitives. This matrix, called *Match (left, right)*, contains all the possible matches between right and left primitives and has dimension $m \times n$. In this matrix, as observed (see Fig. 2), some contours lead to a maximum number of intersections.

But finalizing the correspondence problem between primitives remains impossible. With that objective, the same procedure is applied again, this time from right to left. That is, we carry out the computation of the epipolar line intersections by taking the right image as starting point. The same procedure leads this way to the construction of a second matrix *Match (right, left)* of possible matches. This matrix has dimension $n \times m$. After that, matching can be finalized by searching for corresponding maxima in the two matrices, as indicated in the algorithm given here after and summarizing the whole procedure, including the (standard) 3D reconstruction:

1. Pre-processing of the image data.

- a. Estimation of the epipolar geometry (matrices F and F^t).
- b. Segmentation of the stereo pair of images and construction of the lists of contour points.
- c. Classification of the contour point lists as vertical segments (vertical straight lines), horizontal segments (horizontal straight lines) or arbitrary shaped contours. See Fig. 4.

2. Determination of the (sub-)set of geometric primitives seen in both images, using a priori knowledge (see section 3). See Fig. 7.

Table 1. Matching matrices.

Match (left, right)

	C_{r1}	C_{r2}	C_{r3}	C_{r4}	C_{r5}	C_{r6}	C_{r7}
C_{l1}	342	116	0	0	0	106	97
C_{l2}	75	110	0	0	0	35	35
C_{l3}	0	0	0	141	90	0	26
C_{l4}	0	0	123	0	0	5	5
C_{l5}	0	0	0	94	135	9	26
C_{l6}	300	107	121	0	42	172	210
C_{l7}	304	100	12	76	115	211	218

Match (right, left)

	C_{l1}	C_{l2}	C_{l3}	C_{l4}	C_{l5}	C_{l6}	C_{l7}
C_{r1}	326	114	0	0	0	105	93
C_{r2}	73	105	0	0	0	38	33
C_{r3}	0	0	0	133	0	6	1
C_{r4}	0	0	135	0	87	0	15
C_{r5}	0	0	92	0	129	11	22
C_{r6}	292	99	0	118	35	173	209
C_{r7}	297	106	119	119	116	213	219

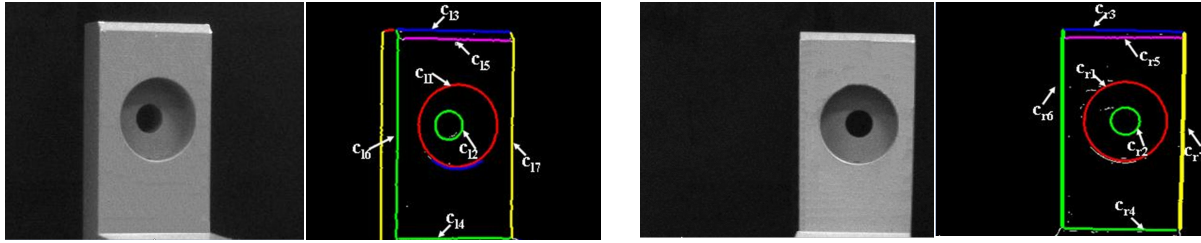


Figure 4. Stereoscopic image pair with edges extracted from both images and grouped to form line segments or arbitrary shaped contours.

3. Determination of the candidate matches.

d. For each left primitive $C_{i,l}$, computation of intersection number $n_{i,l}$ of epipolar lines $l_{i,l}$ with right primitives $C_{j,r}$. The result is the matrix Match (left, right). See Tab 1.

e. For each right primitive $C_{j,r}$, computation of intersection number $n_{j,r}$ of epipolar line $l_{j,r}$ with left primitives $C_{i,l}$ in the other image. The result is the matrix Match (right, left). See Tab 1.

4. Finalization/validation of the matches.

f. Evaluation of a similarity criterion between the two matrices, involving searching for corresponding maxima in the two matrices.

g. Elimination of the contours matched according to step (f) in the two matrices.

h. Repeat steps (d) to (g) until all contours have been processed.

5. 3D Reconstruction. See Fig. 5.

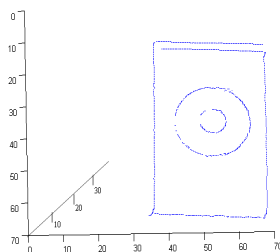


Figure 5. 3D reconstruction of the object.

The matching technique proposed assumes that the contours belonging to the same geometric primitives of the object are present in both images, which is quite restrictive. To deal with the general case, for which some primitives are only present in one image, a classical approach consists in introducing supplementary constraints, such as similarity, exclusivity or proximity

[12]. In our case, as we consider industrial applications such as quality control and since a CAD model is available, it seems natural to use the a priori knowledge provided by the model as a constraint. This is to be described in the next section.

3 Comparison of Real and Conceptual Image Data to Sustain Matching

A complete 3D model is established using the CATIA CAD system (Dassault systems). The approach suggested for selection of the primitives to be firstly matched, secondly reconstructed, consists in comparing real images with conceptual, *i.e.* synthetic images, generated taking into account the view points of the two camera by use of the calibration parameters [13]. The resulting conceptual images (left and right images) are then used as a reference. As a result, introducing a specific coding, these representations highlight the segments, which are visible in both images. As a consequence, only these contours will undergo the matching procedure described in section 2 and the features not visible from the current camera view points “reduced” model of the part, which contains the features visible in the real images (see an example Fig. 6). The corresponding two synthetic views can then be superimposed onto the real ones for the two points of view of the cameras of the stereoscopic acquisition head. This comparison, carried out pixel by pixel, leads to keep only contours common in both images, as shown in Fig. 7. This way, using the “reduced” CAD models, we can correctly match corresponding contours and then reconstruct the object, even when the images do not have the same contour contents. Further, this CAD model plays an important role in our application, as the comparison of real images with their conceptual counterparts enables also performing highly accurate metrology, for *e.g.* quality control [13], [14].

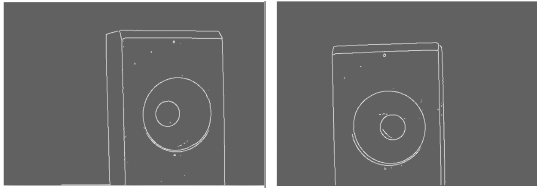


Figure 6. Example of real contour images

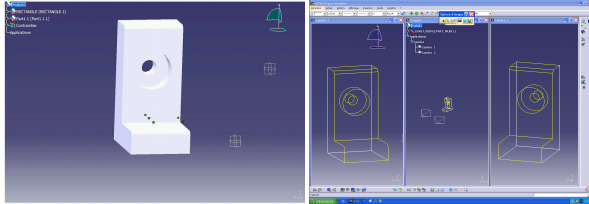


Figure 7. CATIA model (left image) and reduced model (wire-frame) taking the acquisition conditions into account (right image)

4 Conclusion and outlook

In this contribution, we have introduced an original technique for matching contours. The performance of this matching algorithm strongly depends on the estimation of the fundamental matrix and the quality of the segmentation process. Specifically tailored for quasi-polyhedral manufactured parts to allow for the classification of contours with simple geometry (straight segments and arbitrary shaped contours), the matching procedure evaluates “cross-correspondences” established from left to right and vice-versa using so-called “matching matrices”. Base of the approach is also a selection of candidate contours using a comparison between synthetic images, generated with help of a CAD system, and the acquired images. The approach has been tested on various real images and the above experimental results show that our method both produces accurate contour correspondences and an accurate 3D reconstruction. Current work focuses on the combination of surface and contour-based approaches enabling full 3D reconstruction or measurements on industrial objects. For this reason, we relate the 3D contour data to surface data (using a technique described elsewhere), in order to obtain a complete description of the object. The applications considered primarily carry out dimensional analysis of the objects by comparison with their synthetic models. For this purpose we are developing an inspection robot capable of covering a half-sphere of 2m radius. Among the perspectives are:

- the development and installation of the platform for active acquisition and controlled processing of the images, based on conceptual CAD models,
- the integration into the inspection platform of the measuring heads, together with a planning tool using generic Situation Graph Trees, in order to manage several measuring tools
- the evaluation of the images by exploiting, in real time if needed, the same tools as used for simulation to correct processing errors (dynamic re-planning), according to the objective of the application.

References

- [1] R. Hartley and A. Zisserman, “Multiple View Geometry in Computer Vision”, *Cambridge University Press*, 2000.
- [2] N. Ayache and P. T. Sander, “Artificial Vision for Mobile Robots: Stereo Vision and Multisensory Perception”, *MIT Press*, 1991.
- [3] R. Hartley, “Euclidean reconstruction from uncalibrated views” in *Proceedings of the Second Joint European - US Workshop on Applications of Invariance in Computer Vision*, pp. 237-256, 1994.
- [4] N. B. Dinkar, N. Bhat, and K. N. Shree, “Ordinal measures for image correspondence”, *IEEE Transactions on Pattern Analysis and Machine Intelligence*, vol. 20, no. 4, pp. 415-423, 1998.
- [5] S. Sekhavat and A. K. Farhad, “Geometric feature-based matching in stereo images”, in *Proceedings of Information Decision and Control 99*, pp. 65-70, 1999.
- [6] Z. Zhang, “Determining the epipolar geometry and its uncertainty: A review”, *International Journal of Computer vision*, vol. 27, no. 2, pp. 161-198, 1998.
- [7] C. L. Feng and Y. S. Hung, “A robust method for estimating the fundamental matrix”, in *VII Digital Image Computing: Techniques and Applications*, 2003.
- [8] A. Xavier and S. Joaquin, “Overall regarding fundamental matrix estimation”, *Image and vision Computing*, vol. 21, pp. 205-220, 2003.
- [9] S. Joaquin, A. Xavier, and B. Joan, “A comparative review of camera calibrating methods with accuracy evaluation”, *Pattern Recognition*, vol. 35, pp. 1617-1635, 2002.
- [10] C. Daul, “Construction et utilisation de liste de primitives en vue d'une analyse dimensionnelle de pièce à géométrie simple”, *Ph.D. thesis, Université Louis Pasteur de Strasbourg*, 1989.
- [11] M. Xie, “Cooperative strategy for matching multi-level edge primitives”, *Image and Vision Computing*, pp. 89-99, 1995.
- [12] R. Horaud and T. Skordas, “Stereo correspondences through feature grouping and maximal cliques”, *IEEE Transactions on Pattern Analysis and Machine Intelligence*, vol. 11, no. 11, pp. 1168-1180, 1989.
- [13] P. Graebbling, A. Lallement, D.-Y. Zhou, and E. Hirsch, “Optical high precision 3D dimensional vision based quality control of manufactured parts using synthetic images and knowledge for image data evaluation and interpretation”, *Applied Optics : Information processing*, vol. 41, no. 14, pp. 2627-2643, 2002.
- [14] A. Lallement, R. Khemmar, and E. Hirsch, “Automated delineation of regions of interest through adaptive segmentation and interpretation of images in view of dimensional evaluation of manufactured parts”, *Journal of Electronic Imaging*, vol. 13, no. 3, pp. 462-473, 2004.
- [15] A. Xavier, and J. Salvi, “Overall view regarding fundamental matrix estimation”, *Journal of Image and Vision Computing*, vol. 21, no. 2, pp. 205-220, 2003.
- [16] C. Chua, Y. Ho, and Y. liang, “Rejection of mismatched correspondences along the affine epipolar line”, *Journal of Image and Vision Computing*, vol. 18, no. 6, pp. 445-462, 2000.